Journal of Computational Physics 230 (2011) 2021–2030

Contents lists available at ScienceDirect

Journal of Computational Physics

journal homepage: www.elsevier.com/locate/jcp

An iterative method to solve a regularized model for strongly nonlinear long internal waves

Wooyoung Choi [a,b,*], Arnaud Goullet [a], Tae-Chang Jo [c]

[a] Department of Mathematical Science, Center for Applied Mathematics and Statistics, New Jersey Institute of Technology, Newark, NJ 07102-1982, USA
[b] Division of Ocean Systems Engineering, Korea Advanced Institute of Science and Technology, Daejeon 305-701, South Korea
[c] Department of Mathematics, Inha University, Incheon 402-751, South Korea

ARTICLE INFO

Article history:
Received 17 June 2010
Received in revised form 22 November 2010
Accepted 30 November 2010
Available online 13 December 2010

Keywords:
Internal waves
Regularized model
Iterative method

ABSTRACT

We present a simple iterative scheme to solve numerically a regularized internal wave model describing the large amplitude motion of the interface between two layers of different densities. Compared with the original strongly nonlinear internal wave model of Miyata [10] and Choi and Camassa [2], the regularized model adopted here suppresses shear instability associated with a velocity jump across the interface, but the coupling between the upper and lower layers is more complicated so that an additional system of coupled linear equations must be solved at every time step after a set of nonlinear evolution equations are integrated in time. Therefore, an efficient numerical scheme is desirable. In our iterative scheme, the linear system is decoupled and simple linear operators with constant coefficients are required to be inverted. Through linear analysis, it is shown that the scheme converges fast with an optimum choice of iteration parameters. After demonstrating its effectiveness for a model problem, the iterative scheme is applied to solve the regularized internal wave model using a pseudo-spectral method for the propagation of a single internal solitary wave and the head-on collision between two solitary waves of different wave amplitudes.

1. Introduction

Recently nonlinear internal solitary waves propagating in density stratified oceans have attracted much attention and the number of field observations is rapidly increasing [5]. These long internal waves frequently observed in coastal regions are often strongly nonlinear as the wave amplitude is comparable to the characteristic vertical length scale. Therefore, the well-known weakly nonlinear models such as the Korteweg-de Vries (KdV) equation for uni-directional waves and the Boussinesq equations for bi-directional waves commonly used for long surface waves in a homogeneous layer have been found to fail to describe large amplitude internal solitary waves [2,8].

When the density changes rather abruptly over a thin transition layer (called the pycnocline), the stratified ocean is often approximated by two fluid layers of different constant densities for which the higher-order nonlinear dispersive effects can be incorporated into a relatively simple system of nonlinear evolution equations describing the motion of the interface between the two fluid layers [2,10]. Its solitary wave solutions have been found to agree well with laboratory experiments and numerical solutions of the Euler equations [1,2]. Since this strongly nonlinear model neglects the effects of viscosity and a

* Corresponding author at: Department of Mathematical Science, Center for Applied Mathematics and Statistics, New Jersey Institute of Technology, Newark, NJ 07102-1982, USA.
E-mail address: wychoi@njit.edu (W. Choi).

0021-9991/$ - see front matter © 2010 Elsevier Inc. All rights reserved.
doi:10.1016/j.jcp.2010.11.049

thin density transition layer between the two layers, the tangential velocities are discontinuous across the interface and its initial value problem is known to be ill-posed [6,7,9].

To overcome this difficulty, the model has been regularized [3] by changing the short-wave behavior that is insignificant in the long-wave dynamics and, in fact, is modeled incorrectly in the long wave asymptotic model. An attempt to solve the regularized model numerically was made in Choi et al. [3], but it was found desirable to develop a more efficient numerical method due to a more complicated coupling between the upper and lower layers compared with the original strongly nonlinear model.

In this paper, we introduce an iterative scheme to solve the regularized model of Choi et al. [3] and discuss its convergence. After presenting the regularized model in Section 2, we describe the iterative scheme and the result of convergence analysis in Section 3. With choosing an optimum set of iteration parameters, we solve the regularized model numerically for the propagation of a single solitary wave and the asymmetric head-on collision between two solitary waves to demonstrate the effectiveness of the iterative scheme in Section 4.

2. A regularized strongly nonlinear model

A regularized strongly nonlinear internal wave model for a system of two constant-density layers bounded by the upper and lower rigid boundaries can be written [3], in terms of the local layer thicknesses η_i and the horizontal velocities u_i evaluated at the rigid boundaries in the upper ($i = 1$) and lower ($i = 2$) layers, as

$$\eta_{i,t} + \left[\eta_i\left(u_i - \frac{1}{6}\eta_i^2 u_{i,xx}\right)\right]_x = 0, \tag{2.1}$$

$$u_{i,t} + u_i u_{i,x} + g\zeta_x = -\frac{P_x}{\rho_i} + \left[\frac{1}{2}\eta_i^2\left(u_{i,xt} + u_i u_{i,xx} - u_{i,x}^2\right)\right]_x. \tag{2.2}$$

Here the subscripts x and t represent partial differentiation with respect to space and time, respectively, and the local layer thicknesses are defined by

$$\eta_1 = h_1 - \zeta, \quad \eta_2 = h_2 + \zeta, \tag{2.3}$$

where h_i are the undisturbed layer thicknesses and ζ is the displacement of the interface. We remark that the original strongly nonlinear long wave model of Miyata [10] and Choi and Camassa [2] written in terms of the depth-averaged horizontal velocities suffers from Kelvin–Helmholtz (KH) instability due to a velocity discontinuity across the deformed interface. By introducing the horizontal velocities at the upper and lower walls, u_i, it was shown in Choi et al. [3] that the model given by (2.1) and (2.2) suppresses the KH instability when it is linearized. Since the system is written in a conserved form, it has the following obvious conservation laws

$$\frac{\mathrm{d}}{\mathrm{d}t}\int_{-\infty}^{\infty}\zeta \mathrm{d}x = 0, \quad \frac{\mathrm{d}}{\mathrm{d}t}\int_{-\infty}^{\infty}u_i \mathrm{d}x = 0. \tag{2.4}$$

We remark that, for numerical computations, it is convenient to rewrite Eq. (2.2) as

$$\rho_i\left[u_i - \frac{1}{2}(\eta_i^2 u_{i,x})_x\right]_t = -P_x - \rho_i\left[\frac{1}{2}u_i^2 + g\zeta - \frac{1}{2}(\eta_i^2 u_i u_{i,x})_x + \frac{1}{6}\eta_i u_{i,x}(\eta_i^3 u_{i,xx})_x\right]_x, \tag{2.5}$$

where (2.1) has been used for $\eta_{i,t}$. Obviously, the last term on the right-hand side is a asymptotically higher-order term than the remaining terms and could be dropped for consistency. Nevertheless, it is kept here since we would like to solve (2.2) exactly. In terms of the well-posedness of the linearized system, the last term makes no difference since it is a nonlinear term and, therefore, it can be dropped without affecting the well-posedness if one wants to have a model asymptotically equivalent to (2.2).

The system of four equations given by (2.1) and (2.5) for $i = 1$ and 2 can be reduced to a system of two time evolution equations. Choosing (2.1) for $i = 1$ and subtracting (2.5) for $i = 1$ and $i = 2$ to eliminate P yields the following two evolution equations for ζ and V

$$\zeta_t = \left[\eta_1\left(u_1 - \frac{1}{6}\eta_1^2 u_{1,xx}\right)\right]_x, \tag{2.6}$$

$$V_t = \sum_{i=1}^{2}(-1)^i\rho_i\left[\frac{1}{2}u_i^2 + g\zeta - \frac{1}{2}(\eta_i^2 u_i u_{i,x})_x + \frac{1}{6}\eta_i u_{i,x}(\eta_i^3 u_{i,xx})_x\right]_x, \tag{2.7}$$

where $V(x,t)$ is defined by

$$V = \sum_{i=1}^{2}(-1)^{i-1}\rho_i\left[u_i - \frac{1}{2}(\eta_i^2 u_{i,x})_x\right]. \tag{2.8}$$

Once the evolution equations given by (2.6) and (2.7) are integrated in time for ζ and V, the horizontal velocities u_i can be found by solving the following system of coupled differential equations with variable coefficients

$$\eta_1\left[u_1-\frac{1}{6}\eta_1^2u_{1,xx}\right]+\eta_2\left[u_2-\frac{1}{6}\eta_2^2u_{2,xx}\right]=C, \tag{2.9}$$

$$\rho_1\left[u_1-\frac{1}{2}(\eta_1^2u_{1,x})_x\right]-\rho_2\left[u_2-\frac{1}{2}(\eta_2^2u_{2,x})_x\right]=V. \tag{2.10}$$

Notice that η_i in (2.9) and (2.10) are known since ζ is already computed at a new time step. Here, while the second equation is nothing but (2.8), the first Eq. (2.9) is obtained by adding (2.1) for $i = 1$ and 2 to eliminate ζ_t and integrating once in x with an integration constant C, which depends on the boundary conditions. Physically (2.9) implies that the volume flux is independent of x.

When discretized, the system given by (2.9) and (2.10) could be computationally expensive to solve, in particular, for two-dimensional problems unless an efficient numerical scheme is found. Even for one-dimensional problem, if one uses a pseudo-spectral method, the operator becomes a full matrix which is time-consuming to invert at every time step since the operator depends on time. In fact, in Choi et al. [3], a direct inversion method with a second-order finite difference scheme to approximate the operators was adopted to solve (2.9) and (2.10) and found numerically ineffective.

3. An iterative scheme and its convergence

To solve the system given by (2.9) and (2.10) efficiently, we rewrite (2.9) as

$$\eta_1U_1+\eta_2U_2=R_1, \tag{3.1}$$
$$\rho_1U_1-\rho_2U_2=R_2, \tag{3.2}$$

where U_i and R_i are given by

$$U_i=u_i-\alpha_ih_i^2u_{i,xx}, \tag{3.3}$$

$$R_1=C+\sum_{i=1}^{2}\left(\frac{1}{6}\eta_i^3u_{i,xx}-\alpha_i\eta_ih_i^2u_{i,xx}\right), \tag{3.4}$$

$$R_2=V-\sum_{i=1}^{2}(-1)^i\rho_i\left[\frac{1}{2}(\eta_i^2u_{i,x})_x-\alpha_ih_i^2u_{i,xx}\right]. \tag{3.5}$$

In (3.3)–(3.5), notice that terms with constant α_i are introduced to write (3.1) and (3.2) as a system of equations for U_i from which u_i can be easily obtained by inverting the linear operators with constant coefficients given by (3.3). Then, as described in Appendix A, α_i are determined for a new iterative scheme to converge fast and are assumed to be positive so that the operators to be inverted to find u_i from known U_i are positive definite.

Once the right-hand sides R_i are evaluated with the results from the previous iteration step, (3.1) and (3.2) are the linear equations for U_i at the new iteration step, whose expressions in terms of R_i can be found analytically. Then, u_i can be computed by inverting independently for $i = 1$ and $i = 2$ the linear operators with constant coefficients defined in (3.3), as mentioned previously. It is convenient to invert these constant operators, for example, when a pseudo-spectral method is used. On the other hand, if one uses a finite difference method for spatial discretization, the coefficients do not have to be constant. Therefore, $\alpha_ih_i^2$ in (3.3) and (3.5) and $\alpha_i\,\eta_ih_i^2$ in (3.4) can be replaced by $\alpha_i\,\eta_i^2$ and $\alpha_i\eta_i^3$, respectively, and an iterative scheme described below can be applied without any modification. A similar iterative scheme can be used for a system given by (2.9) and (2.10), but, then, u_i have to be solved simultaneously since the terms in the square brackets that appear on the left-hand sides of (2.9) and (2.10) are all different.

3.1. Iterative scheme

For given η_i, the solutions of (3.1) and (3.2) can be obtained by using the following iterative scheme

$$\eta_1U_1^{(n+1)}+\eta_2U_2^{(n+1)}=R_1^{(n)}, \tag{3.6}$$
$$\rho_1U_1^{(n+1)}-\rho_2U_2^{(n+1)}=R_2^{(n)}, \tag{3.7}$$

where $U_i^{(n+1)}$ are U_i at the $(n+1)$th iteration step and $R_i^{(n)}$ are the right-hand sides of (3.1) and (3.2) evaluated with the results from the nth iteration step. Then, $U_i^{(n+1)}$ can be found analytically as

$$U_1^{(n+1)}=\frac{\rho_2R_1^{(n)}+\eta_2R_2^{(n)}}{\rho_1\eta_2+\rho_2\eta_1},\quad U_2^{(n+1)}=\frac{\rho_1R_1^{(n)}-\eta_1R_2^{(n)}}{\rho_1\eta_2+\rho_2\eta_1}. \tag{3.8}$$

Now the equations for the upper and lower layers are decoupled and u_i can be found independently for $i = 1$ and $i = 2$ as

$$u_i^{(n+1)} = \left(1 - \alpha_i h_i^2 \partial_x^2\right)^{-1} U_i^{(n+1)}. \tag{3.9}$$

The operator (3.9) can be easily inverted numerically. For example, for the second-order central difference scheme, a tridiagonal matrix solver can be used and, for a pseudo-spectral method, it is simple division since the operator is independent of space by construction. We emphasize that the operators are rearranged with introducing α_i before any numerical discretization of the original operators is made so that the expressions for U_i can be found analytically, as shown in (3.8). Then, the resulting linear systems with simple operators given by (3.9) are inverted to find u_i without any operator splittings, which are often required for the well-known iterative schemes such as Jacobi or Gauss–Seidel methods.

This iterative scheme is applied repeatedly until the following condition is met

$$\frac{\left|u_i^{(n+1)} - u_i^{(n)}\right|_{\max}}{\left|u_i^{(n)}\right|_{\max}} < \epsilon, \tag{3.10}$$

where we adopt $\epsilon = 1 \times 10^{-12}$ for our computations presented later. Alternatively, we could use a criterion based on the residuals of the discretized linear system given by (3.1) and (3.2) with which we continue the iteration process until the residuals reach a certain tolerance level. As will be discussed in Section 3.3, the criterion given by (3.10) is found more satisfactory and is therefore adopted in this paper.

In the followings, we derive a condition under which the iterative scheme converges for fixed physical parameters (h_i and ρ_i), and show how to choose α_i such that fastest convergence is achieved.

3.2. Convergence

For Fourier analysis, we first linearize the system of (3.1) and (3.2) with assuming that $\zeta/h_i \ll 1$

$$h_1\left(1 - \alpha_1 h_1^2 \partial_x^2\right) u_1^{(n+1)} + h_2\left(1 - \alpha_2 h_2^2 \partial_x^2\right) u_2^{(n+1)} = C + \sum_{i=1}^{2}\left(\frac{1}{6} - \alpha_i\right) h_i^3 u_{i,xx}^{(n)}, \tag{3.11}$$

$$\rho_1\left(1 - \alpha_1 h_1^2 \partial_x^2\right) u_1^{(n+1)} - \rho_2\left(1 - \alpha_2 h_2^2 \partial_x^2\right) u_2^{(n+1)} = V - \sum_{i=1}^{2}(-1)^i \rho_i\left(\frac{1}{2} - \alpha_i\right) h_i^2 u_{i,xx}^{(n)}. \tag{3.12}$$

By substituting the following expression into (3.1) and (3.2)

$$u_i^{(n)} = a_i^{(n)} e^{ikx}, \tag{3.13}$$

where k is the wave number, we have

$$h_1(1 + \alpha_1 k^2 h_1^2) a_1^{(n+1)} + h_2(1 + \alpha_2 k^2 h_2^2) a_2^{(n+1)} = \overline{C} - \sum_{i=1}^{2}\left(\frac{1}{6} - \alpha_i\right) k^2 h_i^3 a_i^{(n)}, \tag{3.14}$$

$$\rho_1(1 + \alpha_1 k^2 h_1^2) a_1^{(n+1)} - \rho_2(1 + \alpha_2 k^2 h_2^2) a_2^{(n+1)} = \overline{V} + \sum_{i=1}^{2}(-1)^i \rho_i\left(\frac{1}{2} - \alpha_i\right) k^2 h_i^2 a_i^{(n)}, \tag{3.15}$$

where $\bar{f}$ represents the Fourier transform of f. For convergence of our iterative scheme, the behavior for large k is crucial (see Appendix A) and, as $k \to \infty$, (3.14) and (3.15) can be approximated to

$$\begin{pmatrix} \alpha_1 h_1^3 & \alpha_2 h_2^3 \\ \alpha_1 \rho_1 h_1^2 & -\alpha_2 \rho_2 h_2^2 \end{pmatrix} \begin{pmatrix} a_1^{(n+1)} \\ a_2^{(n+1)} \end{pmatrix} = \begin{pmatrix} -\left(\frac{1}{6} - \alpha_1\right) h_1^3 & -\left(\frac{1}{6} - \alpha_2\right) h_2^3 \\ -\rho_1\left(\frac{1}{2} - \alpha_1\right) h_1^2 & \rho_2\left(\frac{1}{2} - \alpha_2\right) h_2^2 \end{pmatrix} \begin{pmatrix} a_1^{(n)} \\ a_2^{(n)} \end{pmatrix}, \tag{3.16}$$

which can be re-written as

$$\begin{pmatrix} a_1^{(n+1)} \\ a_2^{(n+1)} \end{pmatrix} = \mathbf{A}(\alpha_1, \alpha_2) \begin{pmatrix} a_1^{(n)} \\ a_2^{(n)} \end{pmatrix}, \tag{3.17}$$

where matrix $\mathbf{A}$ depends on α_i for fixed physical parameters (h_i and ρ_i). For convergence, the absolute values of two eigenvalues of matrix $\mathbf{A}$, $\lambda_{1,2}$, have to be smaller than 1

$$|\lambda_i(\alpha_1, \alpha_2)| < 1, \tag{3.18}$$

which determine the ranges of α_i.

For simplicity, the two fluid densities are assumed to be close to each other so that $\rho_1/\rho_2 \simeq 1$ (relevant for oceanic applications), the matrix $\mathbf{A}$ becomes

$$\mathbf{A} = \frac{1}{h_1 + h_2} \begin{pmatrix} -\left[h_2\left(\frac{1}{2} - \alpha_1\right) + h_1\left(\frac{1}{6} - \alpha_1\right)\right]/\alpha_1 & h_2^3 \big/ (3\alpha_1 h_1^2) \\ h_1^3 \big/ (3\alpha_2 h_2^2) & -\left[h_2\left(\frac{1}{6} - \alpha_2\right) + h_1\left(\frac{1}{2} - \alpha_2\right)\right]/\alpha_2 \end{pmatrix}, \tag{3.19}$$

whose two eigenvalues are given by

$$\lambda_{1,2} = 1 - \frac{\alpha_1(3h_1 + h_2) + \alpha_2(h_1 + 3h_2)}{12\alpha_1\alpha_2(h_1 + h_2)} \pm \frac{\left[(\alpha_1(3h_1 + h_2) - \alpha_2(h_1 + 3h_2))^2 + 16\alpha_1\alpha_2 h_1 h_2\right]^{1/2}}{12\alpha_1\alpha_2(h_1 + h_2)}. \tag{3.20}$$

Then, for convergence of our iterative scheme, we choose α_i for which the maximum of the two eigenvalues has to be less than 1. This happens when the first two terms in (3.20) vanish and the absolute values of the two eigenvalues are the same and less than 1. This requires α_i to satisfy the following relationship

$$\alpha_2 = \frac{(3h_1 + h_2)\alpha_1}{12(h_1 + h_2)\alpha_1 - (h_1 + 3h_2)}. \tag{3.21}$$

From (3.21), since $\alpha_2 > 0$, as mentioned previously, it can be seen that α_1 satisfies the following inequality

$$\alpha_1 > \frac{h_1 + 3h_2}{12(h_1 + h_2)} > 0, \tag{3.22}$$

under which it can be shown that the condition given by (3.18) is always fulfilled. Finally, for optimum values of α_i, we need to choose α_i which makes λ_i as small as possible and the results are

$$\alpha_1 = \frac{h_1 + 3h_2}{6(h_1 + h_2)}, \quad \alpha_2 = \frac{3h_1 + h_2}{6(h_1 + h_2)}. \tag{3.23}$$

Then, the iterative scheme is expected to converge fastest and $|\lambda_i|$ is given by

$$|\lambda_1| = |\lambda_2| = \left[\frac{4h_1h_2}{(3h_1 + h_2)(h_1 + 3h_2)}\right]^{1/2}, \tag{3.24}$$

which is less than 1/2.

Fig. 3.1(a) shows $|\lambda_2|$, for varying α_i, given by (3.20) with a negative sign for the depth ratio of $h_2/h_1 = 3$ while Fig. 3.1(b) shows a region in the (α_1, α_2)-plane where the iterative scheme converges. In the shaded region, both $|\alpha_1|$and $|\alpha_2|$ are less than 1 while $|\alpha_2| > 1$ in the non-shaded region. For the depth ratio of $h_2/h_1 = 3$, the optimum values of α_i indicated by the dot are $\alpha_1 = 5/12$ and $\alpha_2 = 1/4$ from (3.23) and the absolute values of λ_i are $|\lambda_i| = 1/5$.

For the case of arbitrary density ratios, the optimum values of α_i are given in Appendix B with including the effect of finite wave amplitude a, which requires one to change the local thicknesses h_1 and h_2 to $h_1 - a$ and $h_2 + a$, respectively.

3.3. A simple test for convergence

To test the iterative scheme, we consider a model problem similar to (2.9) and (2.10) with $h_1 = 1$, $h_2 = 3$, $\rho_1 = 1$, and $\rho_2 = 1.003$

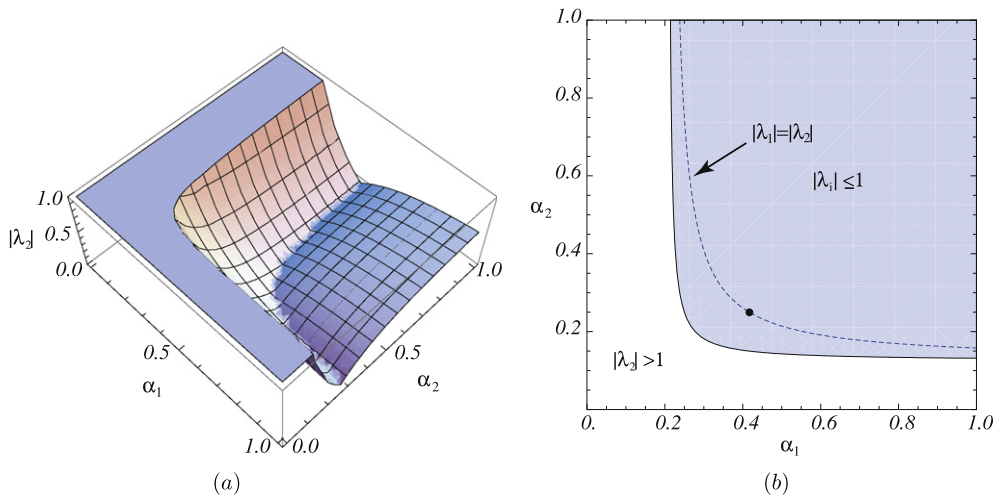

Fig. 3.1. (a) $|\lambda_2|$ given by (3.20) with a negative sign for $h_2/h_1 = 3$. (b) The iterative scheme converges for α_i in a shaded region where $|\lambda_i| < 1$. On the dashed line, the absolute values of two eigenvalues are identical ($|\lambda_1| = |\lambda_2|$). The minimum eigenvalues occur at optimum values of α_i which are given by (3.23) and indicated by the dot in the figure.

Table 3.1
Comparison of the numerical solutions of (3.25) and (3.26) with the exact solutions given by (3.27). Here $N_{\text{iteration}}$ is the number of iterations with tolerance $\epsilon = 10^{-12}$ and e_i are defined as $e_i = |u_{i\text{exact}} - u_{i\text{numerical}}|_{\max}/|u_{i\text{exact}}|_{\max}$. Notice that the optimum values are $\alpha_1 = 5/12$ and $\alpha_2 = 1/4$ and a second-order finite difference scheme has been used for spatial discretization. For $\alpha = 5/24$ and $\alpha_2 = 1/8$, the iterative scheme failed since $|\lambda_2| > 1$.

α_1	α_2	$N_{\text{iteration}}$	$e_1 \times 10^4$	$e_2 \times 10^4$
5/12	1/5	47	2.522198102	2.132061190
5/12	**1/4**	**31**	**2.522198103**	**2.132061190**
5/12	1/3	39	2.522198101	2.132061191
5/12	1/2	58	2.522198092	2.132061192
4/12	1/4	41	2.522198106	2.132061190
5/12	**1/4**	**31**	**2.522198103**	**2.132061190**
6/12	1/4	33	2.522198098	2.132061191
5/12	1/4	37	2.522198101	2.132061191
5/24	1/8	failed		

Table 3.2
Error estimates for varying Δx with the optimum values of α_i given by (3.23).

α_1	α_2	Δx	$N_{\text{iteration}}$	$e_1 \times 10^4$	$e_2 \times 10^4$	$e_1 \sim \Delta x^m$
5/12	1/4	$2\pi/200$	31	2.522198	2.132061	
5/12	1/4	$2\pi/400$	31	0.630483	0.532953	$m = 2.00015$
5/12	1/4	$2\pi/800$	31	0.157616	0.133250	$m = 2.00004$

$$h_1\left(u_1 - \frac{h_1^2}{6}u_{1,xx}\right) + h_2\left(u_2 - \frac{h_2^2}{6}u_{2,xx}\right) = r_1(x), \tag{3.25}$$

$$\rho_1\left(u_1 - \frac{h_1^2}{2}u_{1,xx}\right) - \rho_2\left(u_2 - \frac{h_2^2}{2}u_{2,xx}\right) = r_2(x), \tag{3.26}$$

where $r_1(x)$ and $r_2(x)$ are given by substituting the following exact solutions into the left-hand sides of (3.25) and (3.26), respectively

$$u_{1\,\text{exact}}(x) = \sin(x) + \cos(2x), \quad u_{2\,\text{exact}}(x) = 2\cos(x) + 3\sin(2x), \quad \text{for } 0 \leqslant x \leqslant 2\pi. \tag{3.27}$$

To solve (3.25) and (3.26) using the iterative scheme, we use a second-order finite difference method with $\Delta x = 2\pi/200$ for spatial discretization and $\epsilon = 10^{-12}$. In Table 3.1, the numerical solutions are compared with the exact solutions given by (3.27). Clearly the least number of iterations is required with the optimum values of α_i given by (3.23) and the iterative scheme fails with α_i in a divergent region (the non-shaded region in Fig. 3.1). This indicates that our analysis for $k \to \infty$ presented in Section 3.2 is valid although the maximum wave number resolved in our computations (which is $\pi/\Delta x$) is large, but finite. Since we use a second-order difference approximation, the errors of our numerical solutions are proportional to Δx^2, as shown in Table 3.2. The maximum residuals of the discretized system of (3.25) and (3.26) for our numerical solutions are also computed as 1.332978×10^{-11}, 5.984191×10^{-11}, and 1.962377×10^{-10} for $\Delta x = 2\pi/200$, $2\pi/400$, and $2\pi/800$, respectively. Since the residuals are sensitive to the choice of Δx, a criterion based on the residuals discussed in Section 3.1 seems to be less useful for our iterative scheme.

4. Numerical solutions of the regularized model

To solve the evolution Eqs. (2.6) and (2.7) numerically, we use a fourth-order Runge–Kutta method for time integration and a pseudo-spectral method for spatial discretization. As described in Section 2, once ζ and V are updated at a new time

Table 4.1
Average number of iterations for varying α_i for the propagation of a solitary wave with wave amplitude $a_0 = -0.6$ and physical parameters $(\rho_1, \rho_2, h_1, h_2, g) = (1, 1.003, 1, 3, 1)$. A pseudo-spectral method is used for spatial discretization with $N = 2^9$ and the total domain length is $L = 200$ while a fourth-order Runge–Kutta method is used for time integration with $\Delta t = 0.01$ and $t_{\max} = 1000$.

α_1	0.4	0.6	0.8	**0.938053**	1.0	1.2
$N_{\text{iteration}}$ with $\alpha_2 = 0.192153$	Failed	15	10.5	**10**	10	11
λ_1	0.338	0.395	0.454	0.492	0.447	0.340
λ_2	1.683	0.959	0.626	0.492	0.509	0.558
α_2	0.1	0.15	**0.192153**	0.2	0.25	0.3
$N_{\text{iteration}}$ with $\alpha_1 = 0.938053$	Failed	12.25	**10**	10	10	10.5
λ_1	0.363	0.434	0.492	0.464	0.331	0.253
λ_2	1.284	0.715	0.492	0.503	0.563	0.613

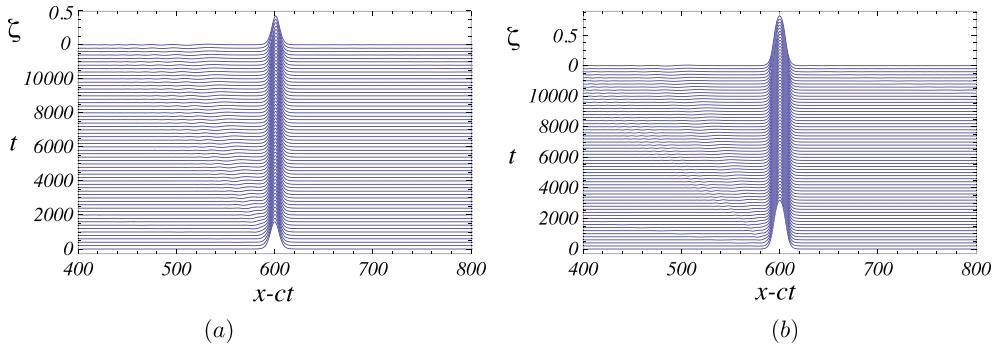

Fig. 4.1. Numerical solutions of the regularized model for a single solitary wave in a reference frame moving with constant speed c. The initial wave profile is the solitary wave solution of the model of Miyata–Choi–Camassa and c is its wave speed. (a) $a = -0.4$ and $c = 0.0522$; (b) $a/h_1 = -0.8$ and $c = 0.0544$.

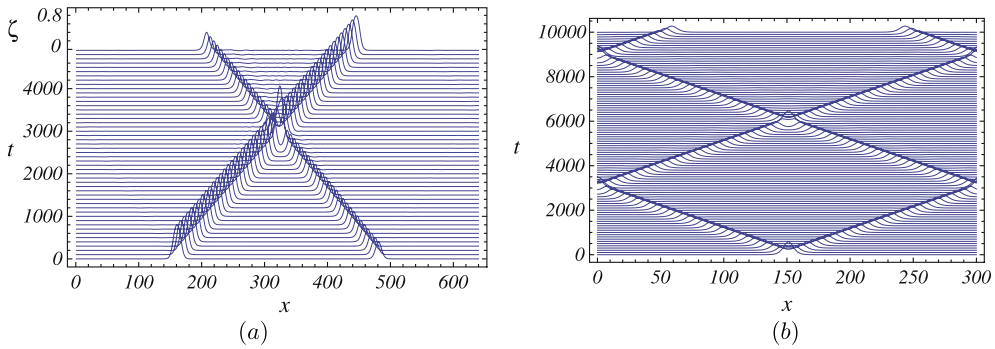

Fig. 4.2. Numerical solutions of the regularized model: (a) Head-on collision of two solitary waves of the Miyata–Choi–Camassa model with amplitudes $a = -0.8$ and $a = -0.4$. (b) Evolution of an initial profile given by $\zeta(x,0) = -0.6\ \mathrm{sech}^2(0.2x)$ with zero horizontal velocity.

step, the horizontal velocities u_1 and u_2 can be found independently by inverting the linear operators with constant coefficients defined in (3.9). This inversion is a simple division in Fourier space such that the Fourier transform of $u_i^{(n+1)}$ can be found as $\hat{u}_i^{(n+1)} = (1 + \alpha_i h_i^2 k^2)^{-1} \hat{U}_i^{(n+1)}$.

To test the iterative scheme, we consider the propagation of a single solitary wave of amplitude $a_0 = -0.6$ of the original model of Miyata[10] and Choi and Camassa [2] with $(\rho_1, \rho_2, h_1, h_2, g) = (1, 1.003, 1, 3, 1)$. It should be emphasized again that the propagation of a single solitary wave cannot be simulated with the original model which is illposed. For these physical parameters, the optimum values for α_i are found, from (B.10) for finite amplitude waves, as $\alpha_1 = 0.938053$ and $\alpha_2 = 0.192153$. In Table 4.1, for varying α_i, we present the average number of iterations necessary for convergence at each substep of the Runge–Kutta method with $\Delta t = 0.01$ satisfying the CFL condition based on the linear long wave speed for $0 \leqslant t \leqslant 1000$. Here, the length of our total computational domain is taken to be $L = 200$ and the number of grid points (Fourier modes) is $N = (5/2) \times 2^9$ among which 2^9 Fourier modes are meaningful since the rest is used to eliminate aliasing errors with considering that the regularized model is the fourth-order nonlinear equations. From Table 4.1, we notice that the fastest convergence is achieved with the optimum values of α_i estimated from (B.10), but the iterative scheme is so effective that a small number of iterations is required even for non-optimum iteration parameters as long as the absolute values of the corresponding eigenvalues are less than one.

Fig. 4.1 shows the long-term numerical solutions of the regularized model (2.1) and (2.2) initialized with the solitary wave solution of the original strongly nonlinear model of Miyata [10] and Choi and Camassa [2] for $0 \leqslant t \leqslant 1.2 \times 10^4$ and $0 \leqslant x \leqslant 1200$ with $\Delta t = 0.1$ and $N = (5/2) \times 2^{10}$. The initial wave amplitudes are $a = -0.4$ and $a = -0.8$ for which the optimum iteration parameters are, from (B.10), $(\alpha_1, \alpha_2) = (0.7509, 0.2130)$ and $(\alpha_1, \alpha_2) = (1.1332, 0.1704)$, respectively. For these numerical computations, the average number of iteration per each time integration is approximately $N_{\text{iteration}} = 9$ for $a = -0.4$ and $N_{\text{iteration}} = 10$ for $a = -0.8$. Compared with the numerical scheme used in Choi et al. [3] where the direct inversion of a linear system is required, the new iterative scheme is found more than 4 times faster. The elapsed computing times for $a = -0.8$ are measured 0.35 s and 1.54 s per time step for the new and old numerical schemes, respectively. Notice that small dispersive waves are shed downstream since the initial wave profile is close to, but not the solution of the regularized model.

To further test the new iterative scheme for more general time-dependent problems, we consider two different initial conditions with $N = (5/2) \times 2^9$ and $\Delta t = 0.01$. Fig. 4.2(a) shows the asymmetric head-on collision between two solitary waves

of the Miyata–Choi–Camassa model of amplitudes −0.8 and −0.4. During the collision, the peak amplitude reaches about −1.263. Here α_i are computed based on the initial amplitude of the larger solitary wave which is much less than the local maximum amplitude of 1.263 during this computation, but the iterative scheme shows no sign of divergence. Fig. 4.2(b) shows the time evolution of an initial profile given by $\zeta(x,0) = -0.6\mathrm{sech}^2(0.2x)$ located at the center of the computational domain with periodic boundary conditions. With $u_i = 0$ at $t = 0$, the initial profile is split into two solitary waves, which propagate in the opposite directions to collide symmetrically at the boundaries of the computational domain. Here we compute α_i based on the initial maximum displacement of the interface so that $(\alpha_1, \alpha_2) = (0.938, 0.192)$.

5. Concluding remarks

We propose an effective iterative method to solve a system of coupled nonlinear evolution equations, regularized to suppress shear instability, for large amplitude long internal waves in a two-layer system. Through linear analysis, a condition for iteration parameters for convergence is provided and tested. It is found that the iterative scheme with the optimum values for fastest convergence is effective in solving the regularized model even when the wave amplitude is large. Although the one-dimensional model is considered in this paper, a similar iterative model can be used to solve the two-dimensional regularized model [4] with bottom topography.

Acknowledgements

WC and AG gratefully acknowledge support from the Office of Naval Research through Grant N00014-08-1-0377 and the WCU (World Class University) program through the National Research Foundation of Korea funded by the Ministry of Education, Science and Technology (R31-2008-000-10045-0). The work of TJ was supported by Basic Science Research Program through the National Research Foundation of Korea funded by the Ministry of Education, Science and Technology (2010-0023265).

Appendix A. Iterative operator inversion

Consider a simple equation for $u(x)$ given by

$$\mathcal{L}[u] \equiv (1 - \partial_x^2)u = f(x), \tag{A.1}$$

where $f(x)$ is a known slowly-varying function. Although (A.1) can be solved analytically, we attempt to solve it numerically to explain our iterative scheme.

Since $u(x)$ is expected to be a slowly varying function and the second term on the left-hand side of (A.1) is supposed to be small compared with the first term, we assume to use the following simple iterative scheme.

$$u^{(n+1)} = f(x) + u_{xx}^{(n)}, \tag{A.2}$$

where $u^{(n)}$ is the estimate at the nth iteration step and $u^{(0)}$ is an initial guess.

In Fourier space, by writing $u^{(n)} = a^{(n)}e^{ikx}$, (A.2) yields an equation for $a^{(n+1)}$

$$a^{(n+1)}(k) = \bar{f}(k) - k^2 a^{(n)} = \bar{f}(k) - k^2\left[\bar{f}(k) - k^2 a^{(n-1)}\right] = \frac{1-(-k^2)^{n+1}}{1-(-k^2)}\bar{f}(k) + (-k^2)^{n+1}a^{(0)}(k). \tag{A.3}$$

For large k, $a^{(n+1)}$ can be approximated by

$$a^{(n+1)}(k) \sim (-k^2)^n \bar{f}(k) + (-k^2)^{n+1}a^{(0)}(k), \tag{A.4}$$

which implies that $a^{(n+1)}(k)$ for large k grows as the number of iteration n increases and the iteration scheme would fail no matter how small $a^{(0)}(k)$ is. This conclusion also holds even for the case of $a^{(0)}(k) = 0$ which is identical to an iteration scheme given by $u^{(n+1)} = \epsilon^2 u_{xx}^{(n)}$ with $u^{(0)} = f(x)$.

To overcome this difficulty, we first replace the iteration scheme, after subtracting αu_{xx} from both sides of (A.1), by

$$u^{(n+1)} - \alpha u_{xx}^{(n+1)} = f(x) + (1-\alpha)u_{xx}^{(n)}, \tag{A.5}$$

where α is a constant to be determined, and then $a^{(n+1)}$ can be found as

$$a^{(n+1)}(k) = \frac{1-[(\alpha-1)k^2/(1+\alpha k^2)]^{n+1}}{1-[(\alpha-1)k^2/(1+\alpha k^2)]}\frac{\bar{f}(k)}{1+\alpha k^2} + \left[\frac{(\alpha-1)k^2}{(1+\alpha k^2)}\right]^{n+1} a^{(0)}(k), \tag{A.6}$$

whose behavior for large k is found to be

$$a^{(n+1)}(k) = \left(\frac{\alpha-1}{\alpha}\right)^{n+1} a^{(0)}(k). \tag{A.7}$$

Then, for convergence, we have the following condition for α

$$\left|\frac{\alpha-1}{\alpha}\right| < 1, \tag{A.8}$$

which yields $\alpha > \frac{1}{2}$. Notice that the case of $\alpha = 1$ corresponds to direct inversion of operator $\mathcal{L}$.

Appendix B. Iteration parameters for arbitrary wave amplitudes and density ratios

We first linearize the system of (3.1) and (3.2) about the maximum displacement from the mean interface (or about $\zeta = a$)

$$\eta_1\left(1-\alpha_1 h_1^2\partial_x^2\right)u_1^{(n+1)} + \eta_2\left(1-\alpha_2 h_2^2\partial_x^2\right)u_2^{(n+1)} = C + \sum_{i=1}^{2}\left(\frac{1}{6}\eta_i^2 - \alpha_i h_i^2\right)\eta_i u_{i,xx}^{(n)}, \tag{B.1}$$

$$\rho_1\left(1-\alpha_1 h_1^2\partial_x^2\right)u_1^{(n+1)} - \rho_2\left(1-\alpha_2 h_2^2\partial_x^2\right)u_2^{(n+1)} = V - \sum_{i=1}^{2}(-1)^i\rho_i\left(\frac{1}{2}\eta_i^2 - \alpha_i h_i^2\right)u_{i,xx}^{(n)}, \tag{B.2}$$

where η_1 and η_2 should be understood as $h_1 - a$ and $h_2 + a$. Then, by substituting into the linearized system

$$u_i^{(n)} = a_i^{(n)} e^{ikx}, \tag{B.3}$$

we have

$$\eta_1(1+\alpha_1 k^2 h_1^2)a_1^{(n+1)} + \eta_2(1+\alpha_2 k^2 h_2^2)a_2^{(n+1)} = \overline{C} - \sum_{i=1}^{2}\left(\frac{1}{6}\eta_i^2 - \alpha_i h_i^2\right)k^2\eta_i a_i^{(n)}, \tag{B.4}$$

$$\rho_1(1+\alpha_1 k^2 h_1^2)a_1^{(n+1)} - \rho_2(1+\alpha_2 k^2 h_2^2)a_2^{(n+1)} = \overline{V} + \sum_{i=1}^{2}(-1)^i\rho_i\left(\frac{1}{2}\eta_i^2 - \alpha_i h_i^2\right)k^2 a_i^{(n)}, \tag{B.5}$$

where $\bar{f}$ represents the Fourier transform of f. For convergence of the iterative scheme, the behavior for large k is crucial and, as $k \to \infty$, this system can be approximated to

$$\begin{pmatrix} \alpha_1\eta_1 h_1^2 & \alpha_2\eta_2 h_2^2 \\ \alpha_1\rho_1 h_1^2 & -\alpha_2\rho_2 h_2^2 \end{pmatrix}\begin{pmatrix} a_1^{(n+1)} \\ a_2^{(n+1)} \end{pmatrix} = \begin{pmatrix} -\eta_1\left(\frac{1}{6}\eta_1^2 - \alpha_1 h_1^2\right) & -\eta_2\left(\frac{1}{6}\eta_2^2 - \alpha_2 h_2^2\right) \\ -\rho_1\left(\frac{1}{2}\eta_1^2 - \alpha_1 h_1^2\right) & \rho_2\left(\frac{1}{2}\eta_2^2 - \alpha_2 h_2^2\right) \end{pmatrix}\begin{pmatrix} a_1^{(n)} \\ a_2^{(n)} \end{pmatrix}, \tag{B.6}$$

which can be written as

$$\begin{pmatrix} a_1^{(n+1)} \\ a_2^{(n+1)} \end{pmatrix} = \mathbf{A}(\alpha_1,\alpha_2)\begin{pmatrix} a_1^{(n)} \\ a_2^{(n)} \end{pmatrix}, \tag{B.7}$$

where matrix $\mathbf{A}$ depending on α_i and physical parameters such as h_i, ρ_i, and the characteristic wave amplitude a is given by

$$\mathbf{A} = \frac{1}{K}\begin{pmatrix} -\alpha_2 h_2^2\left[\rho_1\eta_2\left(\frac{1}{2}\eta_1^2 - \alpha_1 h_1^2\right) + \rho_2\eta_1\left(\frac{1}{6}\eta_1^2 - \alpha_1 h_1^2\right)\right] & \rho_2 h_2^2\eta_2^3\alpha_2/3 \\ \rho_1 h_1^2\eta_1^3\alpha_1/3 & -\alpha_1 h_1^2\left[\rho_2\eta_1\left(\frac{1}{2}\eta_2^2 - \alpha_2 h_2^2\right) + \rho_1\eta_2\left(\frac{1}{6}\eta_2^2 - \alpha_2 h_2^2\right)\right] \end{pmatrix}, \tag{B.8}$$

with $K = \alpha_1\alpha_2 h_1^2 h_2^2(\eta_1\rho_2 + \eta_2\rho_1)$. The eigenvalues of matrix $\boldsymbol{A}$ can be found as

$$\begin{aligned}\lambda_{1,2} = 1 &- \frac{\alpha_1 h_1^2\eta_2^2(3\rho_2\eta_1 + \rho_1\eta_2) + \alpha_2 h_2^2\eta_1^2(\eta_1\rho_2 + 3\eta_2\rho_1)}{12\alpha_1\alpha_2 h_1^2 h_2^2(\eta_1\rho_2 + \eta_2\rho_1)} \\ &\pm \frac{\left[(\alpha_1 h_1^2\eta_2^2(3\rho_2\eta_1 + \rho_1\eta_2) - \alpha_2 h_2^2\eta_1^2(\rho_2\eta_1 + 3\rho_1\eta_2))^2 + 16\alpha_1\alpha_2\rho_1\rho_2 h_1^2 h_2^2\eta_1^3\eta_2^3\right]^{1/2}}{12\alpha_1\alpha_2 h_1^2 h_2^2(\eta_1\rho_2 + \eta_2\rho_1)}.\end{aligned} \tag{B.9}$$

The minimum of $\max_{i\in\{1,2\}}|\lambda_i|$ occurs when

$$\alpha_1 = \frac{\eta_1^2(\rho_2\eta_1 + 3\rho_1\eta_2)}{6h_1^2(\rho_2\eta_1 + \rho_1\eta_2)}, \quad \alpha_2 = \frac{\eta_2^2(\rho_1\eta_2 + 3\rho_2\eta_1)}{6h_2^2(\rho_2\eta_1 + \rho_1\eta_2)}, \tag{B.10}$$

and the corresponding eigenvalue becomes

$$|\lambda_i| = \left[\frac{4\rho_1\rho_2\eta_1\eta_2}{(\rho_2\eta_1 + 3\rho_1\eta_2)(\rho_1\eta_2 + 3\rho_2\eta_1)}\right]^{1/2}, \tag{B.11}$$

which can be shown to be less or equal to 1/2. Therefore, the iterative scheme should converge with the values of α_i given by (B.10) for any wave amplitudes and density ratios. As $a \to 0$ and $\rho_2/\rho_1 \to 1$, notice that (B.10) and (B.11) can be reduced to (3.23) and (3.24), as expected.

References

[1] R. Camassa, W. Choi, H. Michallet, P. Rusas, J.K. Sveen, On the realm of validity of strongly nonlinear asymptotic approximations for internal waves, J. Fluid Mech. 549 (2006) 1–23.
[2] W. Choi, R. Camassa, Fully nonlinear internal waves in a two-fluid system, J. Fluid Mech. 396 (1999) 1–36.
[3] W. Choi, R. Barros, T. Jo, A regularized model for strongly nonlinear internal solitary waves, J. Fluid Mech. 629 (2009) 73–85.
[4] A. Goullet, R. Barros, W. Choi, Two-dimensional evolution of internal solitary waves: a model and its numerical solutions, 2010, in preparation.
[5] K.R. Helfrich, W.K. Melvill, Long nonlinear internal waves, Ann. Rev. Fluid Mech. 38 (2006) 395–425.
[6] T.-C. Jo, W. Choi, Dynamics of strongly nonlinear solitary waves in shallow water, Stud. Appl. Math. 109 (2002) 205–227.
[7] T.-C. Jo, W. Choi, On stabilizing the strongly nonlinear internal wave model, Stud. Appl. Math. 120 (2008) 65–85.
[8] C.G. Koop, G. Butler, An investigation of internal solitary waves in a two-fluid system, J. Fluid Mech. 112 (1981) 225–251.
[9] R. Liska, L. Margolin, B. Wendroff, Nonhydrostatic two-layer models of incompressible flow, Comput. Math. Appl. 29 (1995) 25–37.
[10] M. Miyata, Long internal waves of large amplitude, in: H. Horikawa, H. Maruo (Eds.), Proceedings of the IUTAM Symposium on Nonlinear Water Waves, 1988, pp. 399–406.